Polymorphisms of SLC22A9 (hOAT7) in Korean Females with Osteoporosis

Seong Kyu Ahn[1], Chang Kook Suh[2], and Seok Ho Cha[1]

Departments of [1]Tropical Medicine and Parasitology, [2]Physiology and Biophysics, College of Medicine, Inha University, Incheon 400-712, Korea

Among solute carrier proteins, the organic anion transporters (OATs) play an important role for the elimination or reabsorption of endogenous and exogenous negatively charged anionic compounds. Among OATs, SLC22A9 (hOAT7) transports estrone sulfate with high affinity. The net decrease of estrogen, especially in post-menopausal women induces rapid bone loss. The present study was performed to search the SNP within exon regions of SLC22A9 in Korean females with osteoporosis. Fifty healthy controls and 50 osteoporosis patients were screened for the genetic polymorphism in the coding region of SLC22A9 using GC-clamped PCR and denaturing gradient gel electrophoresis (DGGE). Six SNPs were found on the SLC22A9 gene from Korean women with/without osteoporosis. The SNPs were located as follows: two SNPs in the osteoporosis group (A645G and T1277C), three SNPs in the control group (G1449T, C1467T and C1487T) and one SNP in both the osteoporosis and control groups (G767A). The G767A, T1277C and C1487T SNPs result in an amino acid substitution, from synonymous vs nonsynonymous substitution arginine to glutamine (R256Q), phenylalanine to serine (F426S) and proline to leucine (P496L), respectively. The Km values and Vmax of the wild type, R256Q, P496L and F426S were 8.84, 8.87, 9.83 and 12.74 μM, and 1.97, 1.96, 2.06 and 1.55 pmol/oocyte/h, respectively. The present study demonstrates that the SLC22A9 variant F426S is causing inter-individual variation that is leading to the differences in transport of the steroid sulfate conjugate (estrone sulfate) and, therefore this could be used as a marker for certain disease including osteoporosis.

Key Words: SLC22A9, Polymorphism, Osteoporosis, Estrone sulfate, Denaturing gradient gel electrophoresis, GC-clamp

INTRODUCTION

Bone is a very complicated tissue in which formation and resorption occur by a bone remodeling process. The loss of bone mass occurs in osteoporosis. Due to low bone mass, there is increased bone fracture of hip, shoulder, wrist and spine. Estrogen is the key hormone for maintaining bone mass. It has been thought that estrogen deficiency is the major cause of age-related bone loss in humans [1]. Osteoporosis is initiated by the failure to acquire the optimal peak of bone mass during growth and/or to maintain bone mass in later years [2]. The rapid loss of bone mass occurs in post-menopausal women, mainly due to the net decrease of estrogen [2]. The estrogen deficiency also induces an imbalance in bone remodeling, accelerates the loss of bone mass increasing fracture risk [3,4]. Therefore, estrogen deficiency can be characterized by high bone turnover with enhanced osteoclastic bone resorption. The important factor in determining bone density and bone turnover in humans is circulating estradiol [5-9]. The most abundant estrogen precursor in circulation is the sulfate conjugate form of estrogen such as estrone sulfate. The amount of this conjugated form of estrogen is several fold higher than that of unconjugated estrogens [10-12]. In addition, the estrone sulfate is well known as the substrate of organic solute carriers such as SLC22A8 (hOAT3), SLC2A9 (hOAT7) and SLC22A11 (hOAT4) [13-15].

The single non-synonymous SNPs (nsSNPs) contribute commonly to the functional diversity on encoded proteins in humans. It appears that nsSNP often lead to unexpected responses to drugs and changes in the susceptibility to disease [16]. A number of reports indicated that nsSNPs affect the functional roles of certain proteins in gene regulation by altering DNA and transcription factor binding and/or by affecting signal transduction [17-19].

ABBREVIATIONS: SLC, solute carrier; OAT, organic anion transporter; DGGE, denaturing gradient gel electrophoresis; SNP, single nucleotide polymorphism.

In this report we screened SNPs of SLC22A9 in two groups of Korean women: one group had osteoporosis and the second was a normal control group. We then performed a functional analysis of the nsSNP from the osteoporosis group by expression in *Xenopus* oocytes.

METHODS

Materials

Taq DNA polymerase and polymerase chain reaction (PCR) primers were purchased from ELPIS BIO (Daejeon, Korea) and Bioneer (Daejeon, Korea), respectively. Restriction enzymes, oligo (dT), LA Taq DNA polymerase and dNTPs were bought from TaKaRa Korea Biomedical Co. (Seoul, Korea), and rNTP and $m^7G(5')ppp(5')G$ Cap analogue for synthesis of cRNA were purchased from Amersham Pharmarcia Biotech (Sunnyvale, CA, USA). T7 RNA polymerase was bought from Stratagene Cloning Systems Inc. (La Jolla, CA, USA) and RNasin (RNA inhibitor) was purchased from Promega (Madison, WI, USA). The DNA blood mini kit was purchased from Qiagen (Hilden, Germany). [^{3}H]estrone sulfate (53 Ci/mmol) was purchased from NEN Life Science Products, Inc. All other chemicals utilized in this study were insured for the highest purity available from commercial sources.

Patients

Blood samples were taken from 50 osteoporosis patients and 50 normal control subjects, which were approved by the Samsung Hospital Institutional Review Board (Cheil General Hospital & Women's Healthcare Center IRB). All subjects involved in the present study were age matched (40 to 65 years of age). The blood samples were kindly supplied from Dr. Ki Ok Han and also employed previous research [20].

PCR reaction

Genomic DNAs were extracted and used as template for the PCR reaction. The PCR primers were approximately 18 mers and were before/after each exon with the GC clamp on the forward or reverse primer [21]. Each PCR reaction mixture (final volume of 12.5 μl) contained 50 ng of iso-lated genomic DNA, 0.5 mM of dNTP, 10 pmol of each primer and 1 unit of DNA taq polymerase. Amplification was performed using a Takara thermocycler (TP-3000) and the PCR cycling conditions were as follows: an initial denaturation at 94°C for 2 min, followed by 30 or 35 cycles of denaturation at 94°C for 1 min, annealing for 1 min at 55°C to 60°C, and elongation at 72°C for 1 min. The last cycle was followed by an additional elongation step of 72°C for 10 min. For optimal DGGE analysis, amplification was followed by a heteroduplexing step, which includes denaturation at 98°C for 10 min, renaturation for 30 min at the annealing temperature of amplification, and extension at 37°C for 10 min. The amplified products were checked by electrophoresis using 1.5 μl (about 1% of total volume) of each product in a 1% agarose gel stained with 1 μg/ml of ethidium bromide solution. The primer sequences and annealing temperature are shown in Table 1.

Denaturing gradient gel electrophoresis (DGGE)

DGGE was performed using a V20-HCDC unit (www.scie-plas.com). PCR products were loaded onto a 230×250 mm, 0.5 mm-thick polyacrylamide gel (acrylamide: bisacrylamide, 37.5:1) containing linear denaturing gradients (100% UF=7 M urea/40% deionized formamide) [22,23]. The percentage of polyacrylamide was 10% and UF solution gradient was from 10% to 70%. Electrophoresis was performed in TAE buffer (40 mM Tris, 20 mM Acetic acid and 1 mM EDTA) at 250 V for 3.5 h at 60°C. The gels were stained with ethidium bromide solution (1 μg/ml) for 10 min and photographed under an UV transilluminator.

DNA sequencing and variant confirmation

Samples showing aberrant DGGE bending patterns were used in PCR with non-GC clamp primers prior or after 80 base pairs of the designated site. Samples showing additional heteroduplex bands were subjected to sequencing analysis for the exact determination of the sequence variant.

Mutant construction

The wild type SLC22A9 cDNA was obtained by screening a human kidney cDNA library and subcloned to pcDNA 3.1(+). In order to prepare mutants SLC22A9, a modified

Table 1. Oligonucleotide primers for PCR amplification of the individual exons of the SLC22A9 gene

Exon No.	Primer sequence		Annealing Temp. (°C)	Cycle	Size (bp)
	Forward	Reverse			
1	Clamp-ATC AAC TGT TCA ACC TCA	ACG AGA ACA GAG CCT CTT AC	60	30	490
2	TGG CTT CCT TCT CTT CCA G	Clamp-TGT TCC ATA CAC ACT CAC	60	30	191
3	Clamp-ACC TGT TTC TGT TTC TCA G	TCC AAA GTG TTG GCT TAC	60	35	242
4	Clamp-ATC TGT TTT TTC TTC CAG	AGA AGA AAC AAA CTC ATA C	57	35	256
5	Clamp-TTC TCT TCC TTG GTC AG	AGC TCC CAT CCA GCT CAC	60	30	209
6	Clamp-TTT CTG CTA TTG TTG AAG	ACA CTG CAT GAA GCT TAC	60	30	205
7	Clamp-TCC TTT TTA ATC ATC ACA G	ACC TGT GAT CTT TTC TCA C	60	30	303
8	Clamp-TGT TCT TCC TTT CTC CAG	AGG GCA TAC TTA AGG TTC TGT AC	60	30	200
9	Clamp-TGC TGT TTC CAC TCA AAG	ACC GGG CTA TTT ACT CAC	60	30	290
10	TCT TTG TAT TTG TTC TAG	Clamp-CCT TGT TAT TTA TTT TC	55	35	227

Clamp sequence: CGC CCG CCG CGC CCC GCG CCC GTC CCG CCG CCC CCG CCC G+TAA TAA TAA T.

Table 2. Oligonucleotide primers for mutant construct preparation of the SLC22A9 gene

Mutant	Primer name	Sequence (5'→3')
G767A	ApaI forward	aat gac act g<u>gg gcc c</u>tc agc c
	PvuII reverse (mutation)	ac<u>c agc tgg</u> agg ata tgc cag tct **T**ga atg gc
T1277C	NdeI forward	aca tgc cca a<u>ca tat g</u>ta aaa gga tct ccc
	reverse-1 (mutation)	aaa cct cac gca gcg tct gca ttt ctt gtg gca ca**G** ata tga tgg cca gaa ggc
	revers-2	att ggc aag agc aga cgc tcc taa gcc cag tgt tgc caa aac ctc acg c
	XmnI reverse-3	tgg gaa tta ctt cat ttc cat ggg caa aag caa ggg tat tgg caa gag cag acg c
C1487T	XmnI forward-1	aat <u>gaa gta att c</u>cc acc ata atc agg gca aga gct atg ggg atc aat gca acc
	forward-2	ggg atc aat gca acc ttt gct aat ata gca gga gcc ctg gct ccc ctc atg atg atc c
	forward-3 (mutation)	tcc cct cat gat gat cct aag tgt gta ttc tcc ac**T** cct gcc ctg gat cat cta tgg
	BamHI reverse	ttc cac tct c<u>gg atc c</u>tc ttg ctt tgg

Restriction enzyme sites and mutated nucleotide were denoted by underline and bold capital letters, respectively.

PCR was performed using primer sets containing both mutation and restriction enzyme sites (Table 2). PCR was sequentially performed for 12 cycles with the first primer (0.5 μM, 1 μl) and 12 cycles with the second primer (0.5 μM, 1 μl) and finally 35 cycles with the third primer (10 μM, 1 μl). The PCR product was sub-cloned using the TA cloning vector (Invitrogen) and confirmed its nucleotide sequences. The mutant constructs were prepared by substituting the mutated product into the wild type cDNA of SLC22A9 using the appropriate restriction enzyme digested cDNA.

cRNA synthesis and uptake experiments using Xenopus laevis oocytes

cRNA synthesis and uptake experiments were performed as described previously [24]. The capped cRNAs were synthesized *in vitro* with T7 polymerase from plasmid cDNAs linearized with *Xho I*. Defolliculated oocytes were injected with 25 ng of the capped cRNAs and incubated in Barth's solution (88 mM NaCl, 1 mM KCl, 0.33 mM Ca(NO$_3$)$_2$, 0.4 mM CaCl$_2$, 0.8 mM MgSO$_4$, 2.4 mM NaHCO$_3$, and 10 mM Hepes) containing 50 μg/ml gentamycin and 2.5 mM pyruvate, pH 7.4, at 18°C. After incubation for 2~3 days, uptake experiments were performed at room temperature in ND96 solution (96 mM NaCl, 2 mM KCl, 1.8 mM CaCl$_2$, 1 mM MgCl$_2$, and 5 mM Hepes, pH7.4). The uptake reaction was initiated by replacing ND96 solution containing various concentrations of radio-labeled estrone sulfate, which was terminated by the addition of sufficient ice-cold ND96 solution followed by five times washing after 1 h incubation. Oocytes were solubilized with 10% SDS and the radioactivity was determined by scintillation counting.

RESULTS

Genomic organization of human SLC22A9

Using the SLC22A9 cDNA nucleotide sequence, we could find the SLC22A9 genomic DNA was from the NCBI database (gi|568815587:63369670-63410919 Homo sapiens chromosome 11, GRCh38 Primary Assembly). The gene, ~41.3 kb long, is located on chromosome 11q13.1. Using the cloned SLC22A9 with the reported genomic sequence, an alignment of the nucleotide sequence was performed to determine the exon-intron gene organization. The SLC22A9 gene consists of 9 introns and 10 exons (Fig. 1). The size
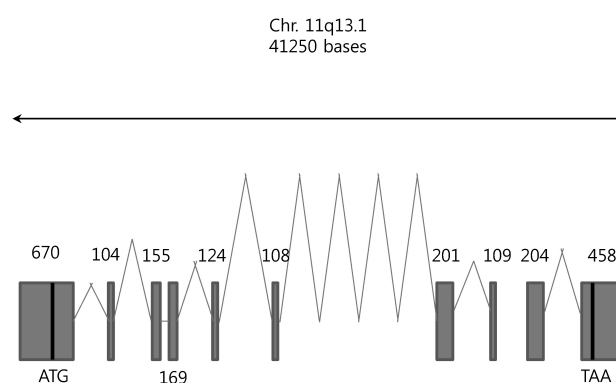

Fig. 1. The exon-intron organization of the SLC22A9 genome and its relationship to the SLC22A9 cDNA. Gray boxes represent the protein-coding regions of the exons.

of each exon, intron, and nucleotide sequence of the splice junction is shown in Table 3. The consensus sequences for RNA splicing (gt/ag) are found in the 5' and 3' termini for each intron. The translation start codon (ATG) is present in exon 1, and the translation termination codon (TAG) is present in exon 10.

GC-clamp PCR, DGGE assay and screening for sequence variation

The DGGE method was used in order to determine the SNP. The PCR conditions were tested over several annealing temperatures and cycle numbers using normal human chromosomal DNA. The typical patterns of each PCR products with synonymous and non-synonymous mutations found using GC-clamping primer sets separated on 1% agarose gel are presented in Fig. 2A. The representative results of DGGE separated on acrylamide gel using several control samples are shown in Fig. 2B. The results of DGGE showed a single band in the SNP found in exons.

To determine the SNP in Korean osteoporosis patients, 50 blood samples were obtained from osteoporosis and normal subjects and screened. When the osteoporosis and control subjects were analyzed, six subjects showed different electrophoretic patterns (Fig. 2C). In general, PCR products were produced in accordance with the different number of bands indicating that a mutation may have occurred.

Table 3. Exon-intron boundaries of the SLC22A9 gene

Exon			Intron					Exon	
No.	Size (bp)	3' junction	5' junction	Size (bp)	No.	3' junction		5' junction	No.
1	670	⋯CGTGACTGAG	**gt**aagaggct⋯	676	1	⋯tctcttcc**ag**		TGGGATCTGG⋯	2
2	104	⋯TATCAGACAG	**gt**gatgtgtg⋯	2405	2	⋯tgtttctc**ag**		GTTTGGGAGA⋯	3
3	155	⋯ATTATGTTAA	**gt**aagccaac⋯	95	3	⋯tttcttcc**ag**		TAGCCGAGTG⋯	4
4	169	⋯TGACCTCAAG	**gt**atgagttt⋯	1582	4	⋯ccttggtc**ag**		TTGGCTGCTA⋯	5
5	124	⋯AACCCTGGAG	**gt**gagctgga⋯	6390	5	⋯attgttga**ag**		ATTTTGAAAT⋯	6
6	108	⋯CCTTTACGAG	**gt**aagcttca⋯	24230	6	⋯atcatcac**ag**		ATTTGCAAAG⋯	7
7	201	⋯GTGCCACAAG	**gt**gagaaaag⋯	1414	7	⋯ctttctcc**ag**		AAATGCAGAC⋯	8
8	109	⋯CCATAATCAG	**gt**acagaacc⋯	455	8	⋯ccactcaa**ag**		GGCAAGAGCT⋯	9
9	204	⋯AGAAAAATGA	**gt**gagtaaat⋯	922	9	⋯tttgttct**ag**		GAGAAAAGAC⋯	10
10	458	⋯AAAAAAAAAA							

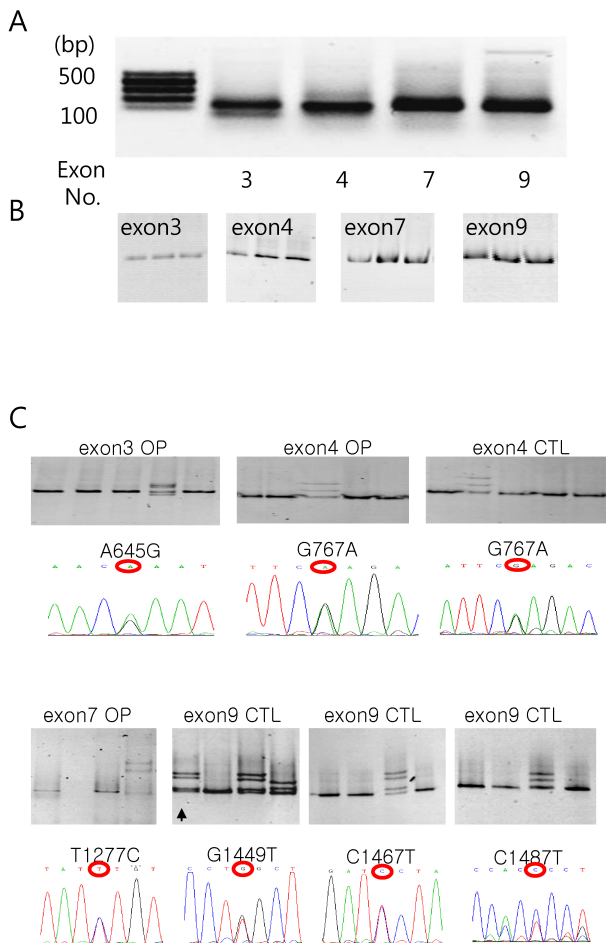Bold **gt** and **ag** were consensus sequences for RNA splicing.

Fig. 2. The typical band patterns of agarose or acrylamide gel electrophoresis. (A) Normal individual genomic DNA amplified using DGGE primer sets for the respective mutation found in exons by duplex PCR. (B) The duplex PCR products from the same genomic DNAs were loaded on a polyacrylamide gel. (C) The aberrant band patterns and sequencing electropherograms of observed SLC22A9 SNPs in osteoporosis and normal subjects. The synonymous A645G, G1449T and C1467T were found in exon 3 and 9, respectively. The G767A, T1277C and C1487T were found in exon 4, 7 and 9, respectively.
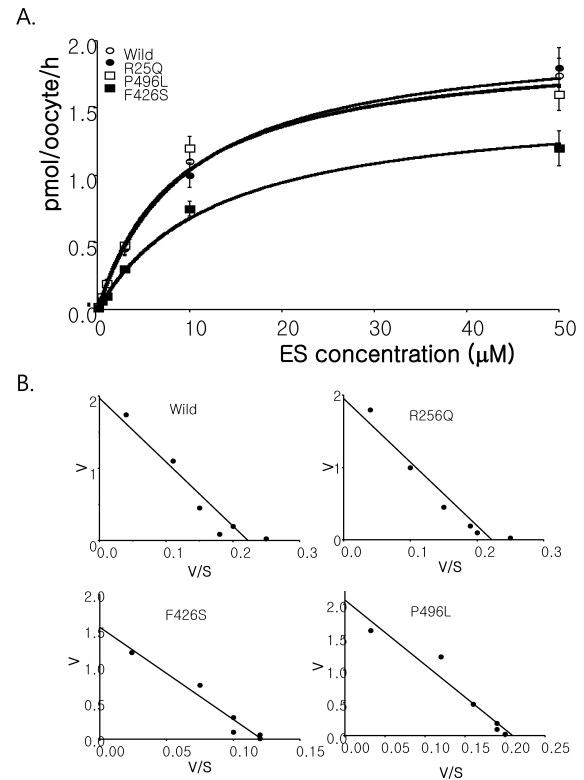

Fig. 3. Transport activity of the SLC22A9 and its variants. (A) Concentration dependence of estrone sulfate mediated by wild type SLC22A9 and variants in *Xenopus laevis* oocytes. Defolliculated stage VI and V oocytes were injected with 25 ng/oocyte of wild-type and variants cRNAs, and incubated for 3 days in Barth's solution at 18°C. After three days, [^{3}H] estrone sulfate uptake experiment was performed using various concentrations (25 nM~50 μM). Each point employs 8~10 oocytes and represented mean±standard error of three independent experiments. (B) Eadie-Hofstee plot analysis for determination of Km and Vmax values.

Among these six SNPs, two SNPs were found in osteoporosis patients (one in exon 3 and the other in exon 7), three SNPs were found in exon 9 of normal subject and one SNP was found in both osteoporosis patients and normal subjects (exon 4). In order to further clarify this, nucleotide sequencing was performed. As shown in Fig. 2C, the SNPs found from exon 5, 7 and 9 showed that G in the 767th nucleotide of the coding region was changed to A (arginine to glutameine), T in the 1277th nucleotide of the coding region was changed to C (phenylalanine to serine) and C in the 1487th nucleotide of the coding region was changed to T (proline to leucine), respectively. However, other SNPs did not change the amino acid sequences.

Functional analysis of human SLC22A9 variant in Xenopus oocytes

In order to examine whether the SLC22A9 polymorphism found in Korean osteoporosis patients affects the functional activity on substrate transport, we constructed mutant cDNAs and expressed them into *Xenopus* oocytes. As shown in Fig. 3, F426S exhibited reduced uptake for [^{3}H] estrone sulfate compared with that of the wild-type SLC22A9. R256Q and P496L did not show a statistically significant change in [^{3}H] estrone sulfate compared with those of the wild-type SLC22A9. According to the changes of concentration-dependent [^{3}H] estrone sulfate in wild type and F426S, the Km values for wild-type and F426S were 0.7 and 1.2 μM, respectively, and the Vmax values for wild-type and F426S were 1.8 and 0.47 pmol/oocyte/h, respectively (Fig. 3).

DISCUSSION

In the present study, the genetic feature of the SLC22A9 was investigated in the Korean women osteoporosis patients and normal subjects. We identified six SNPs (A645G, G767A, T1277C, G1449T, C1467T and C1487T) of SLC22A9 coding region from the osteoporosis and control subjects. Totally 3082 SNPs are reported in the National Center for Biotechnology Information (NCBI) data base. Among them, 1,335 synonymous and non-synonymous SNPs are observed in coding regions. They consist of 68 missense mutations and three stop codon gained mutation within the coding region. Two nsSNP, T1277C (F426S) and C1487T (P496L) of SLC22A9, ares not yet reported in the NCBI data base. We also verify the existence of a functional alteration in F426S.

Human SLC22A9, a sulfate conjugate transporter, transports estrone- and dehydroepiandrosterone sulfate as predominant substrates. In two separate studies, Grumbach and Bilezikian showed estrogen plays a major role in the control of bone growth as well as in the accumulation and maintenance of bone mass. This was shown in using a knockout mouse model that contained mutations impairing estrogen action or formation [25,26]. Bone mass reaches a peak in adults in their twenties and thirties. It begins to decline from age 35~40. The levels of dehyroepiandrosterone and its sulfate conjugate, precursors of androgens and estrogens, decline 2% per year, leaving a residual of 10~20% of the peak production by the eighth decade of life. The age-associated decrease may lead to osteoporosis. Therefore, it is important to understand steroid or steroid conjugate transporter in HRT.

Numerous large-scale screening were carried out to identify genetic variations that affect disease susceptibility and drug response as well as to determine the variants contributing to alter the phenotype. We found three nsSNPs from 50 Korean women osteoporosis patients and normal controls. Unfortunately, there is no information of any functional analysis with discovered nsSNP. Our functional analysis showed the increased value in Km (wild type, 8.84 μM vs. F426S, 12.74 μM) and decreased value in Vmax (wild type, 1.97 pmol/oocyte/h vs. F426S, 1.55 pmol/oocyte/h) in estrone sulfate transport. The transporting activities of the other two nsSNPs (R256Q and P496L) are similar to those of wild type SLC22A9.

In human, the functional properties of transport have been reported. With respect to substrate specificity, hOAT3 (SLC22A8) and hOAT4 (SLC22A11) also transport estrone and dehyroepiandrosterone sulfate. The differences between hOAT3, hOAT4 and SLC22A9 are the expression pattern in organ. The expression of OAT3 was observed in brain, skeletal muscle and kidney [13]. The OAT4 message was observed in kidney and placenta [15]. In contrast, SLC22A9 was expressed exclusively in liver [14]. The result of our ongoing study using Saos-2 and MG-63 osteosarcoma cell line showed the expression of SLC22A11 (hOAT4) and SLC22A9 (hOAT7) by polymerase chain reaction (data not shown). From these results, it might be thought of as indirect evidence of steroid sulfate conjugate transport in bone. When we screened the SNPs of SLC22A8 using the same patient blood samples, no nsSNP was found. In the case of SLC22A11 (hOAT4), we have found one nsSNP and have reported the functional change of transporting activity of the mutant (E278K) in independent osteoporosis patients [20]. In order to understand the characteristics of SLC22A8, 9 and 11, the study using cells derived from primary cultured or immortalized cells was necessary.

Several transporter proteins such as the multidrug resistance associated protein [27,28], organic anion transporting polypeptide C [29,30], Na$^+$-taurocholate cotransporting polypeptide [31,32] and the breast cancer resistance protein (BCRP/ABCG2) [33,34] also transport steroids or their sulfate conjugates and their nsSNPs also showed a decrease of their substrate transporting abilities [35-38]. It has also reported that nsSNPs showing altered activity in some transporters is co-related with certain disease [39,40].

In addition, several reports revealed that some SNPs of SLC22A8 and SLC22A11 are located in the promoter site [41]. NCBI data base also shows some upstream SNP. The study on the regulatory effect of upstream SNP will be also necessary.

In conclusion, we reported for the first time the nsSNPs of SLC22A9 in Korean women with osteoporosis and verified altered activity that may contribute to understanding certain diseases including osteoporosis.

REFERENCES

1. **Riggs BL, Khosla S, Melton LJ 3rd.** Sex steroids and the construction and conservation of the adult skeleton. *Endocr*

Rev. 2002;23:279-302.

2. **Bonjour JP, Theintz G, Law F, Slosman D, Rizzoli R.** Peak bone mass: facts and uncertainties. *Arch Pediatr.* 1995;2:460-468.

3. **Boyle WJ, Simonet WS, Lacey DL.** Osteoclast differentiation and activation. *Nature.* 2003;423:337-342.

4. **Wang FS, Ko JY, Lin CL, Wu HL, Ke HJ, Tai PJ.** Knocking down dickkopf-1 alleviates estrogen deficiency induction of bone loss. A histomorphological study in ovariectomized rats. *Bone.* 2007;40:485-492.

5. **Muir M, Romalo G, Wolf L, Elger W, Schweikert HU.** Estrone sulfate is a major source of local estrogen formation in human bone. *J Clin Endocrinol Metab.* 2004;89:4685-4692.

6. **Slemenda CW, Longcope C, Zhou L, Hui SL, Peacock M, Johnston CC.** Sex steroids and bone mass in older men. Positive associations with serum estrogens and negative associations with androgens. *J Clin Invest.* 1997;100:1755-1759.

7. **Khosla S, Melton LJ 3rd, Atkinson EJ, O'Fallon WM, Klee GG, Riggs BL.** Relationship of serum sex steroid levels and bone turnover markers with bone mineral density in men and women: a key role for bioavailable estrogen. *J Clin Endocrinol Metab.* 1998;83:2266-2274.

8. **Compston JE.** Sex steroids and bone. *Physiol Rev.* 2001;81:419-447.

9. **Hui SL, Perkins AJ, Zhou L, Longcope C, Econs MJ, Peacock M, McClintock C, Johnston CC Jr.** Bone loss at the femoral neck in premenopausal white women: effects of weight change and sex-hormone levels. *J Clin Endocrinol Metab.* 2002;87:1539-1543.

10. **Noel CT, Reed MJ, Jacobs HS, James VH.** The plasma concentration of oestrone sulphate in postmenopausal women: lack of diurnal variation, effect of ovariectomy, age and weight. *J Steroid Biochem.* 1981;14:1101-1105.

11. **Roberts KD, Rochefort JG, Bleau G, Chapdelaine A.** Plasma estrone sulfate levels in postmenopausal women. *Steroids.* 1980;35:179-187.

12. **Hawkins RA, Oakey RE.** Estimation of oestrone sulphate, oestradiol-17beta and oestrone in peripheral plasma: concentrations during the menstrual cycle and in men. *J Endocrinol.* 1974;60:3-17.

13. **Cha SH, Sekine T, Fukushima JI, Kanai Y, Kobayashi Y, Goya T, Endou H.** Identification and characterization of human organic anion transporter 3 expressing predominantly in the kidney. *Mol Pharmacol.* 2001;59:1277-1286.

14. **Shin HJ, Anzai N, Enomoto A, He X, Kim do K, Endou H, Kanai Y.** Novel liver-specific organic anion transporter OAT7 that operates the exchange of sulfate conjugates for short chain fatty acid butyrate. *Hepatology.* 2007;45:1046-1055.

15. **Cha SH, Sekine T, Kusuhara H, Yu E, Kim JY, Kim DK, Sugiyama Y, Kanai Y, Endou H.** Molecular cloning and characterization of multispecific organic anion transporter 4 expressed in the placenta. *J Biol Chem.* 2000;275:4507-4512.

16. **Deighton CM, Walker DJ, Griffiths ID, Roberts DF.** The contribution of HLA to rheumatoid arthritis. *Clin Genet.* 1989;36:178-182.

17. **Firestein GS.** Evolving concepts of rheumatoid arthritis. *Nature.* 2003;423:356-361.

18. **Klareskog L, Padyukov L, Lorentzen J, Alfredsson L.** Mechanisms of disease: Genetic susceptibility and environmental triggers in the development of rheumatoid arthritis. *Nat Clin Pract Rheumatol.* 2006;2:425-433.

19. **Masi AT, Aldag JC, Chatterton RT.** Sex hormones and risks of rheumatoid arthritis and developmental or environmental influences. *Ann N Y Acad Sci.* 2006;1069:223-235.

20. **Lee WK, Kwak JO, Hwang JS, Suh CK, Cha SH.** Identification and characterization of single nucleotide polymorphisms of SLC22A11 (hOAT4) in Korean women osteoporosis patients. *Mol Cells.* 2008;25:265-271.

21. **Mumm S, Jones J, Finnegan P, Henthorn PS, Podgornik MN, Whyte MP.** Denaturing gradient gel electrophoresis analysis of the tissue nonspecific alkaline phosphatase isoenzyme gene in hypophosphatasia. *Mol Genet Metab.* 2002;75:143-153.

22. **Wu Y, Hayes VM, Osinga J, Mulder IM, Looman MW, Buys CH, Hofstra RM.** Improvement of fragment and primer selection for mutation detection by denaturing gradient gel electrophoresis. *Nucleic Acids Res.* 1998;26:5432-5440.

23. **Van Orsouw NJ, Vijg J.** Design and application of 2-D DGGE-based gene mutational scanning tests. *Genet Anal.* 1999;14:205-213.

24. **Kwak JO, Kim HW, Oh KJ, Kim DS, Han KO, Cha SH.** Co-localization and interaction of organic anion transporter 1 with caveolin-2 in rat kidney. *Exp Mol Med.* 2005;37:204-212.

25. **Grumbach MM, Auchus RJ.** Estrogen: consequences and implications of human mutations in synthesis and action. *J Clin Endocrinol Metab.* 1999;84:4677-4694.

26. **Bilezikian JP.** Sex steroids, mice, and men: when androgens and estrogens get very close to each other. *J Bone Miner Res.* 2002;17:563-566.

27. **Evseenko DA, Paxton JW, Keelan JA.** ABC drug transporter expression and functional activity in trophoblast-like cell lines and differentiating primary trophoblast. *Am J Physiol Regul Integr Comp Physiol.* 2006;290:R1357-1365.

28. **Evseenko DA, Murthi P, Paxton JW, Reid G, Emerald BS, Mohankumar KM, Lobie PE, Brennecke SP, Kalionis B, Keelan JA.** The ABC transporter BCRP/ABCG2 is a placental survival factor, and its expression is reduced in idiopathic human fetal growth restriction. *FASEB J.* 2007;21:3592-3605.

29. **Briz O, Serrano MA, MacIas RI, Gonzalez-Gallego J, Marin JJ.** Role of organic anion-transporting polypeptides, OATP-A, OATP-C and OATP-8, in the human placenta-maternal liver tandem excretory pathway for foetal bilirubin. *Biochem J.* 2003;371:897-905.

30. **Patel P, Weerasekera N, Hitchins M, Boyd CA, Johnston DG, Williamson C.** Semi quantitative expression analysis of MDR3, FIC1, BSEP, OATP-A, OATP-C,OATP-D, OATP-E and NTCP gene transcripts in 1st and 3rd trimester human placenta. *Placenta.* 2003;24:39-44.

31. **Ugele B, St-Pierre MV, Pihusch M, Bahn A, Hantschmann P.** Characterization and identification of steroid sulfate transporters of human placenta. *Am J Physiol Endocrinol Metab.* 2003;284:E390-398.

32. **Trauner M, Boyer JL.** Bile salt transporters: molecular characterization, function, and regulation. *Physiol Rev.* 2003;83:633-671.

33. **Evseenko DA, Paxton JW, Keelan JA.** Independent regulation of apical and basolateral drug transporter expression and function in placental trophoblasts by cytokines, steroids, and growth factors. *Drug Metab Dispos.* 2007;35:595-601.

34. **Wang H, Wu X, Hudkins K, Mikheev A, Zhang H, Gupta A, Unadkat JD, Mao Q.** Expression of the breast cancer resistance protein (Bcrp1/Abcg2) in tissues from pregnant mice: effects of pregnancy and correlations with nuclear receptors. *Am J Physiol Endocrinol Metab.* 2006;291:E1295-1304.

35. **Nozawa T, Minami H, Sugiura S, Tsuji A, Tamai I.** Role of organic anion transporter OATP1B1 (OATP-C) in hepatic uptake of irinotecan and its active metabolite, 7-ethyl-10-hydroxycamptothecin: in vitro evidence and effect of single nucleotide polymorphisms. *Drug Metab Dispos.* 2005;33:434-439.

36. **Ho RH, Leake BF, Roberts RL, Lee W, Kim RB.** Ethnicity-dependent polymorphism in Na+-taurocholate cotransporting polypeptide (SLC10A1) reveals a domain critical for bile acid substrate recognition. *J Biol Chem.* 2004;279:7213-7222.

37. **Conrad S, Kauffmann HM, Ito K, Deeley RG, Cole SP, Schrenk D.** Identification of human multidrug resistance protein 1 (MRP1) mutations and characterization of a G671V substitution. *J Hum Genet.* 2001;46:656-663.

38. **Lee SS, Jeong HE, Yi JM, Jung HJ, Jang JE, Kim EY, Lee SJ, Shin JG.** Identification and functional assessment of BCRP polymorphisms in a Korean population. *Drug Metab Dispos.* 2007;35:623-632.

39. **Keitel V, Nies AT, Brom M, Hummel-Eisenbeiss J, Spring H, Keppler D.** A common Dubin-Johnson syndrome mutation impairs protein maturation and transport activity of MRP2 (ABCC2). *Am J Physiol Gastrointest Liver Physiol.* 2003;284:G165-174.

40. **Jamroziak K, Balcerczak E, Smolewski P, Robey RW, Cebula B, Panczyk M, Kowalczyk M, Szmigielska-Kapłon A, Mirowski M, Bates SE, Robak T.** MDR1 (ABCB1) gene polymorphism C3435T is associated with P-glycoprotein activity in B-cell chronic lymphocytic leukemia. *Pharmacol Rep.* 2006;58:720-728.

41. **Ogasawara K, Terada T, Motohashi H, Asaka J, Aoki M, Katsura T, Kamba T, Ogawa O, Inui K.** Analysis of regulatory polymorphisms in organic ion transporter genes (SLC22A) in the kidney. *J Hum Genet.* 2008;53:607-614.